 https://doi.org/10.24191/jeesr.v29i1.026

Sensitivity Analysis on Paper-Based Coplanar Waveguide Antenna-Based Sensor for Hydration Monitoring

Aiza Mahyuni Mozi, Ahmad Rashidy Razali*, Nurul Huda Abdul Rahman, Saidatul Norlyana Azemi, Amirudin Ibrahim, Najwa Mohd Faudzi and Aslina Abu Bakar

Abstract— **Hydration monitoring through non-invasive sweat analysis has gained increasing interest due to its importance in healthcare and wearable sensing applications. This work presents a compact paper-based coplanar waveguide (CPW) antenna-based sensor for hydration monitoring using a controlled sweat droplet deposition approach. Artificial sweat samples representing four hydration states namely hydrated, intermediate, dehydrated, and severely dehydrated were prepared with controlled NaCl concentrations to emulate variations in electrolyte content. The antenna-based sensor performance was experimentally evaluated under one-, two-, and three-droplet conditions to examine the effects of sweat composition and deposited volume. Reflection-coefficient measurements exhibit resonant frequency shifts across hydration levels, with higher salinity sweat producing larger frequency deviations due to stronger electromagnetic loading at the antenna-based sensor sensing region. Both frequency shift (FS) and percent relative frequency shift (PRFS) increase consistently with droplet count for all sweat categories, demonstrating sensitivity to changes in sweat volume and ionic concentration. Under the three-droplet condition, a maximum PRFS of 38.63% is achieved for severely dehydrated sweat. Sensitivity analysis further indicates strong responsiveness at low sweat volumes, with a peak sensitivity of 15.74 GHz mL^{-1} observed under single-droplet loading for severely dehydrated conditions. These results demonstrate effective sensitivity and reliable hydration discrimination, supporting sweat-based hydration monitoring applications.**

Index Terms—CPW antenna-based sensor, frequency shift, hydration monitoring, sweat sensing.

This manuscript is submitted on January 15, 2026, revised on May 21, 2026, accepted on June 24, 2026 and published on October 31, 2026.

Aiza Mahyuni Mozi, Ahmad Rashidy Razali, Amirudin Ibrahim, Najwa Mohd Faudzi and Aslina Abu Bakar are from Faculty of Electrical Engineering, Universiti Teknologi MARA, Permatang Pauh Campus, Pulau Pinang, Malaysia.

Nurul Huda Abdul Rahman is from the Microwave Research Institute, Universiti Teknologi MARA, Shah Alam, Selangor, Malaysia & Faculty of Electrical Engineering, Universiti Teknologi MARA, Shah Alam, Selangor, Malaysia.

Saidatul Norlyana Azemi is from the Faculty of Intelligent Computing, Universiti Malaysia Perlis (Unimap), Perlis

*Corresponding author
Email address: ahmad073@uitm.edu.my

1985-5389/© 2026 The Authors. Published by UiTM Press. This is an open access article under the CC BY-NC-ND license (http://creativecommons.org/licenses/by-nc-nd/4.0/).

I. INTRODUCTION

The healthcare sector has seen significant advancements with the emergence of non-invasive wearable devices that enable continuous health monitoring, providing essential information about individuals' lifestyles and health conditions for accurate assessments [1-4]. These innovations are driving a shift from a hospital-centered approach, which focuses on diagnosis and treatment, to a person-centered healthcare system that emphasizes prevention and early detection of health risks [5-9]. Among these developments, hydration monitoring stands out for its potential to improve personal health and reduce healthcare costs by providing continuous insights into an individual's hydration status through non-invasive sweat analysis [10-12].

Sweat, a hypotonic fluid secreted by eccrine glands in daily amounts of 500–700 ml depending on environmental conditions [13], is easily accessible on the skin surface and contains valuable physiological information. Its composition includes electrolytes such as sodium and potassium, and metabolites including lactate and glucose [14-16]. This composition makes sweat a valuable biofluid for non-invasive health assessments, offering a more practical alternative to other biofluids like saliva and tears. Saliva, while sharing many biological markers with blood, suffers from variability and handling issues that affect reliability [17-20], whereas tears face challenges related to rapid evaporation and user discomfort during sampling [21]. In contrast, sweat's accessibility and composition make it particularly suitable for integration into wearable monitoring systems that track hydration levels [22-23].

Building on these advantages, hydration status represents a critical health parameter that can be effectively assessed through continuous sweat-based evaluation. An imbalance in hydration, particularly dehydration, is characterized by disrupted electrolyte balance, which can impair physiological functions and lead to severe health complications [24-25]. Continuous hydration monitoring therefore plays a vital role in preventing such conditions, offering real-time data to help maintain optimal health. Despite this importance, existing clinical approaches still rely largely on blood and urine analysis, which remain impractical for continuous or real-time assessment [26-27]. Although wearable health-monitoring technologies have advanced considerably, there remains a notable gap in research focused on antenna-based sensors

specifically designed for sweat-based hydration assessment [28-29].

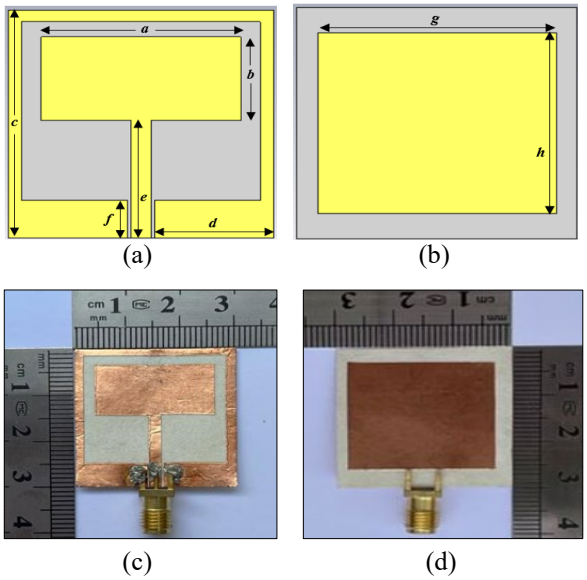
While this gap has motivated several investigations into antenna-based designs, most previous studies have explored microstrip patch antenna-based sensor for hydration monitoring, including approaches with varied dielectric constant and integrated slots for sweat analysis [30-32]. While promising, these approaches often result in bulky and inflexible designs, limiting the comfort and effectiveness for continuous wear. Moreover, the sensitivity of these antenna-based sensors to subtle changes in hydration levels remains underexplored, reducing the overall reliability in detecting sweat composition [33-36].

To address these limitations, this paper proposes a compact CPW antenna-based sensor with a partial reflector, designed to enhance sensitivity and flexibility for continuous hydration monitoring. The research aims to develop a flexible and sensitive antenna-based sensor capable of detecting subtle variations in the dielectric properties of sweat associated with different hydration levels, thereby providing a more reliable solution for non-invasive hydration assessment. The design and fabrication of the CPW antenna-based sensor, along with the preparation of artificial sweat samples, are detailed in the methodology section. Performance characterization through reflection coefficient analysis is combined with sensitivity evaluation using both simulations and experimental measurements, demonstrating the capability of the CPW antenna-based sensor to accurately distinguish hydration levels.

II. Materials and Methods

This section outlines the design and development process of the CPW antenna-based sensor, the preparation of artificial sweat, and the approach utilized for sweat sensing. The detailed methodology provides the foundation for understanding the antenna-based sensor's performance in detecting hydration levels.

A. Design and Development of the CPW Antenna-based Sensor



(a) (b)

(c) (d)

Fig. 1. Proposed CPW antenna-based sensor: (a) front view, (b) back view, (c) fabricated front view, and (d) fabricated back view.

Fig. 1 illustrates the design configuration and fabricated CPW antenna-based sensor operating at a frequency of 2.4 GHz, developed using CST Microwave Studios with an overall dimension of 30 mm x 30 mm. The CPW antenna-based sensor includes a conducting copper strip feedline connected to a rectangular patch, while a ground plane surrounds the patch and runs parallel to the strip on both sides, separated by a narrow slit. The design also incorporates a partial reflector at the bottom layer to suppress backward radiation, thereby improving antenna-based sensor directivity and gain. Filtered paper is used as the substrate material due to its excellent absorbency and flexibility. With a low dielectric constant and a thickness of 0.22 mm, it is particularly suited for sweat sensing hydration monitoring applications, as it efficiently absorbs sweat while maintaining structural flexibility and is economically viable. An SMA connector is connected to the 50 Ω microstrip feedline. The dimensions of the antenna-based sensor design are specified in Table I .

TABLE I. Design Parameters for CPW Antenna-Based Sensor

Parameters	Value (mm)	Parameters	Value (mm)
a	22.5	e	15.5
b	11	f	5
c	30	g	25.5
d	13.5	h	23.5

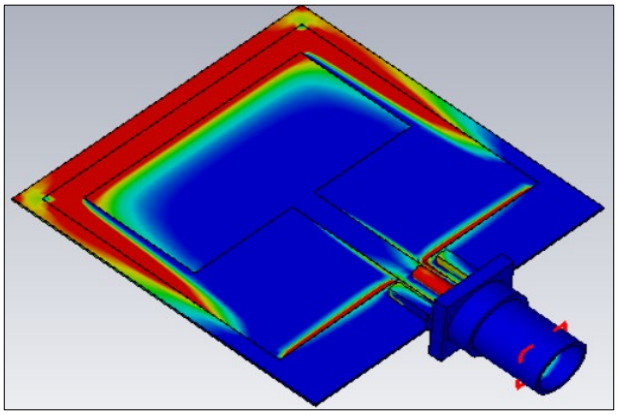


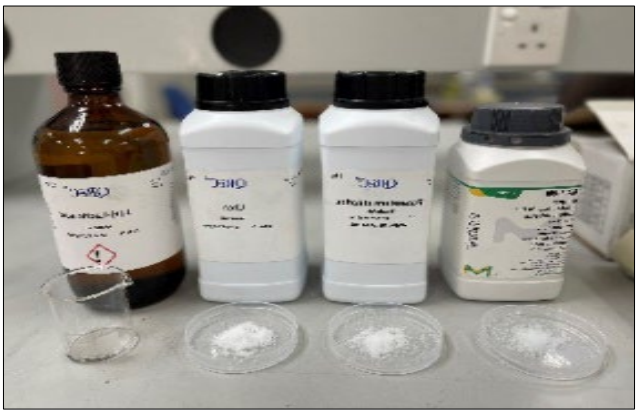
Fig. 2. Simulated electric-field distribution of the proposed CPW antenna-based sensor at 2.4 GHz.

To further validate the sensing behaviour of the proposed structure, the electric-field distribution was simulated to identify the region of maximum field interaction. Fig. 2 presents the simulated electric-field distribution of the proposed CPW antenna-based sensor at 2.4 GHz. The strongest electric field is concentrated along the upper coplanar gap between the patch and the surrounding ground plane, indicated by the red region in the CST plot. This region corresponds to a high-impedance zone where the electric field magnitude $|E|^2$ is maximised,

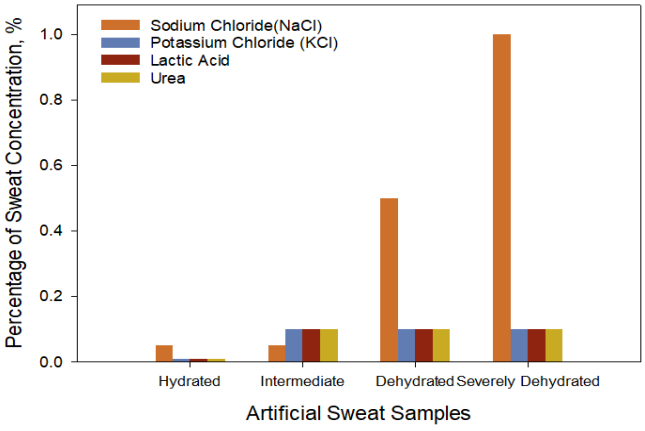
making it highly responsive to changes in the surrounding dielectric environment.

Based on this electric field distribution, sweat droplets are deposited directly on this high-field zone, referred to as the sweat deposition region. Positioning the droplets at this location ensures maximum interaction with the concentrated electric field lines, thereby producing stronger perturbations in the effective permittivity and more pronounced shifts in the resonant frequency. This behaviour is consistent with previously reported CPW-based sensing structures, where field-enhanced sensing at the gap region leads to improved detection performance [37-38]. The experimental sweat-deposition procedure based on this identified sensing region is described in Section C.

B. Preparation and Composition of Artificial Sweat



(a)



(b)

Fig. 3. Artificial sweat preparation: (a) chemical components and (b) percentage composition of artificial sweat formulations.

Sweat is a clear, hypotonic biofluid produced by eccrine and apocrine glands located in the epidermis of the human skin [39-40] . To validate that the artificial sweat closely replicates the ionic composition of natural human sweat, its preparation adheres to the EN1811:2011 European Standard [34], [41]. The formulation process involves the precise dissolution of sodium chloride (NaCl), potassium chloride (KCl), lactic acid and urea in distilled water, as depicted in Fig. 3(a). The percentage concentrations of these chemical components are presented in Fig. 3(b), resulting in four artificial sweat formulations that represent different hydration states: hydrated, intermediate, dehydrated, and severely dehydrated. The dielectric constant of each sweat category was characterized using an open-ended coaxial dielectric probe connected to a vector network analyzer (VNA), as shown in Fig. 4. The measured dielectric constant exhibited clear variations across hydration levels. At 2.4 GHz, hydrated and intermediate sweat recorded dielectric constant of 76.23 and 73.80, respectively, whereas dehydrated and severely dehydrated sweat showed lower values of 63.59 and 51.04, as presented in Fig. 5. These variations arise primarily from differences in NaCl concentration, which affect ionic polarization and electrical conductivity.

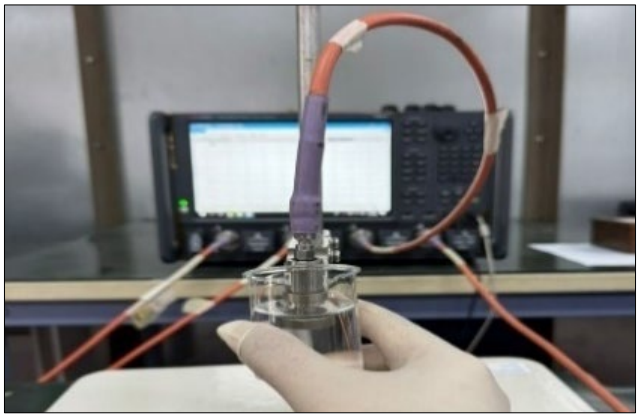


Fig. 4. Dielectric constant measurement setup for artificial sweat samples.

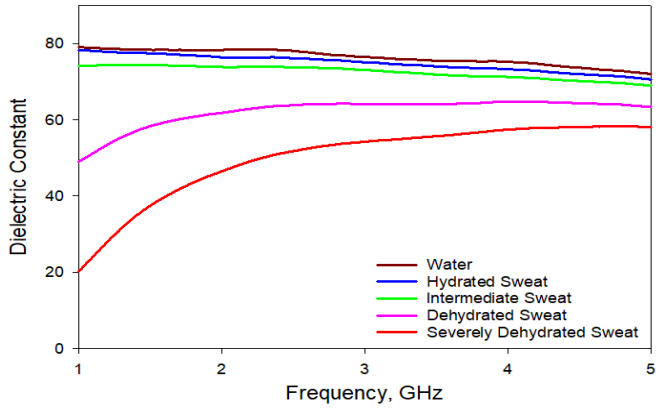


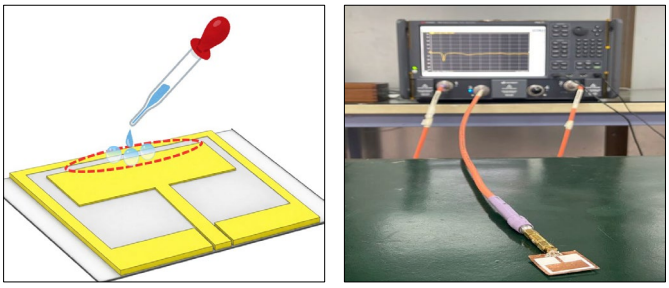
Fig. 5. Dielectric constant of water and artificial sweat samples.

C. Sweat Sensing for Hydration Monitoring

Experimental measurements were conducted using the droplet-based approach to evaluate the sensitivity of the CPW antenna-based sensor for hydration monitoring. The dry condition served as the baseline representing the antenna-based sensor response prior to sweat exposure, while the wet condition corresponded to the antenna-based sensor after controlled droplet deposition of artificial sweat. In this approach, one-, two-, and three-droplets, each with a volume of 0.05 millilitres, were sequentially applied. Each sweat category was evaluated independently, with droplets dispensed onto the

sweat deposition region. Following each deposition, the reflection coefficient was recorded after a two-second interval using the VNA, as illustrated in Fig. 6(a) and Fig. 6(b). This short interval was selected to ensure a stabilized electromagnetic response, enabled by the rapid absorbency of the paper substrate.

Following each measurement, the substrate was allowed to fully dry before proceeding to the next droplet count ensuring that the one-droplet, two-droplet, and three-droplet conditions produced independent and non-cumulative responses. This protocol was applied for all sweat categories to maintain measurement consistency. Selected experiments were repeated under identical testing conditions to verify measurement consistency, and comparable resonant frequency trends were observed across repeated tests. Throughout the experiments, the deposited sweat volume, droplet placement location, and measurement interval were kept constant. To minimise evaporation effects, the reflection coefficient was recorded within two seconds after droplet deposition. All measurements were conducted under laboratory conditions and completed within a short duration to reduce the influence of environmental variations such as temperature and humidity on the antenna-based sensor response. This droplet-based methodology provides precise control of sweat volume and placement, enabling consistent interaction between the deposited sweat and the antenna-based sensor sensing region. The resulting frequency shifts between the dry and wetted states were analysed to evaluate the capability of the CPW antenna-based sensor in distinguishing different hydration levels.



(a) (b)

Fig. 6. Droplet-based sweat measurement procedure: (a) sweat droplet deposition on CPW antenna-based sensor sensing region and (b) reflection coefficient measurement setup.

III. Results and Discussions

This section presents a comprehensive analysis of the measurement results for the proposed CPW antenna-based sensor. The discussion is structured into three parts. The first outlines the baseline characteristics of the antenna-based sensor under dry conditions. The second examines the antenna-based sensor response to different hydration levels based on resonant frequency variation. The third focuses on the evaluation of sensitivity and comparative analysis with previous studies to assess the overall performance of the proposed CPW antenna-based sensor.

A. Performance Characterization under Dry Condition

The performance of the CPW antenna-based sensor is characterized by analyzing its reflection coefficient, gain, and radiation efficiency under dry conditions. These parameters establish the baseline for assessing the antenna-based sensor performance in the absence of sweat exposure. Fig. 7 presents both the simulated and measured reflection coefficients for the CPW antenna-based sensor in dry conditions. The simulation results indicate a reflection coefficient of -36.42 dB at 2.4 GHz, signifying highly efficient power transmission with minimal reflection. The measured reflection coefficient, also at 2.4 GHz, shows a slightly higher value of -27.3 dB, suggesting a slight variation but still demonstrating effective performance. Fig. 8 illustrates the simulated gain and radiation efficiency. The antenna-based sensor demonstrates effective focusing of electromagnetic energy, achieving a gain of 2.15 dBi, while the radiation efficiency of 80.4% indicates its efficiency in converting power into radiated waves.

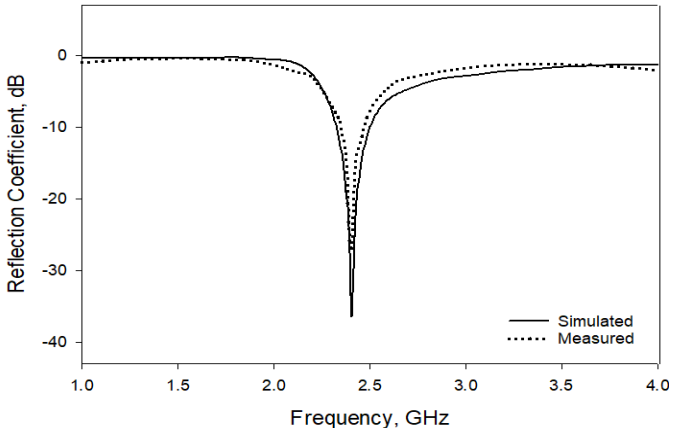


Fig. 7. Simulated and measured reflection coefficient of the CPW antenna-based sensor under dry conditions.

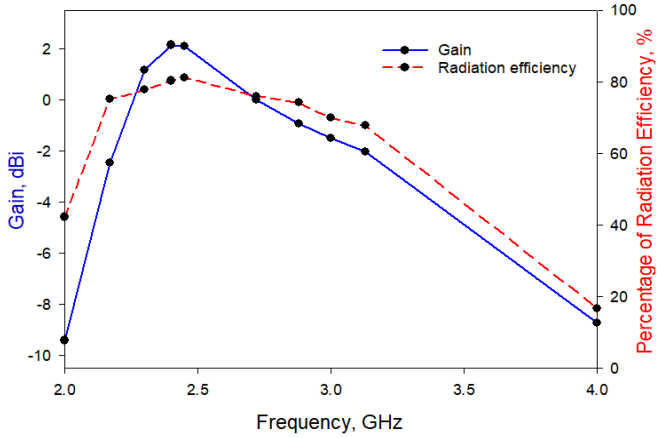


Fig. 8. Simulated gain and efficiency of the CPW antenna-based sensor under dry conditions.

B. Frequency Response to Different Hydration Levels

The sensing performance of the CPW antenna-based sensor was evaluated through the analysis of reflection coefficient responses under incremental droplet application. Each measurement condition, one-, two-, and three-droplets corresponds to a controlled sweat volume deposited on the sensing surface to examine the antenna-based sensor's ability to detect changes in hydration levels. The reflection coefficient responses corresponding to the four sweat categories: hydrated, intermediate, dehydrated, and severely dehydrated sweat, are

presented in Fig. 9, Fig. 10, and Fig. 11, which illustrate the antenna-based sensor behavior under one, two, and three-droplet conditions, respectively. The detailed resonant frequencies and corresponding reflection coefficient magnitudes are summarized in Table II.

The performance of the CPW antenna-based sensor is evaluated using three key parameters: frequency shift (FS), percent relative frequency shift (PRFS), and sensitivity (S), which are calculated using (1)-(3), respectively [42].

$$FS = F_{rd} - F_{rw}\ (GHz) \tag{1}$$

$$PRFS = \frac{F_{rd}-F_{rw}}{F_{rd}}\ x\ 100\ (\%) \tag{2}$$

$$S = \frac{F_{rd}-F_{rw}}{|V_d - V_w|} \tag{3}$$

where F_{rd} denotes the resonant frequency under dry conditions without sweat exposure, and F_{rw} denotes the resonant frequency after sweat deposition. FS, calculated using (1) represents the absolute change in resonant frequency induced by the presence of sweat, while PRFS, calculated using (2) normalizes this change with respect to the dry-state resonant frequency. The sensitivity, S, calculated using (3) is defined as the resonant frequency shift per unit deposited sweat volume, where V_d and V_w represent the deposited sweat volumes under the dry and wetted conditions, respectively. In this study, V_d = 0mL corresponds to the dry state, while V_w corresponds to the deposited sweat volume of 0.05, 0.10, or 0.15 mL for the one-, two-, and three-droplet conditions, respectively. Specifically, S quantifies the change in resonant frequency resulting from an incremental increase in sweat volume applied to the sensing region. This definition directly reflects the antenna-based sensor's responsiveness to variations in sweat loading under the droplet-based measurement approach and provides a practical metric for evaluating hydration sensing performance.

TABLE I I. RESONANT FREQUENCIES OF REFLECTION COEFFICIENT OF THE CPW ANTENNA-BASED SENSOR

		Measurement	
Droplet Conditions	Sweat Concentration	Frequency (GHz)	Reflection Coefficient (dB)
1	Hydrated	1.866	-22.54
	Intermediate	1.820	-30.15
	Dehydrated	1.705	-19.83
	Severely Dehydrated	1.613	-27.9
2	Hydrated	1.774	-22.56
	Intermediate	1.728	-15.09
	Dehydrated	1.636	-25.90
	Severely Dehydrated	1.544	-29.89
3	Hydrated	1.719	-32.53
	Intermediate	1.659	-25.10
	Dehydrated	1.567	-13.84
	Severely Dehydrated	1.473	-22.01

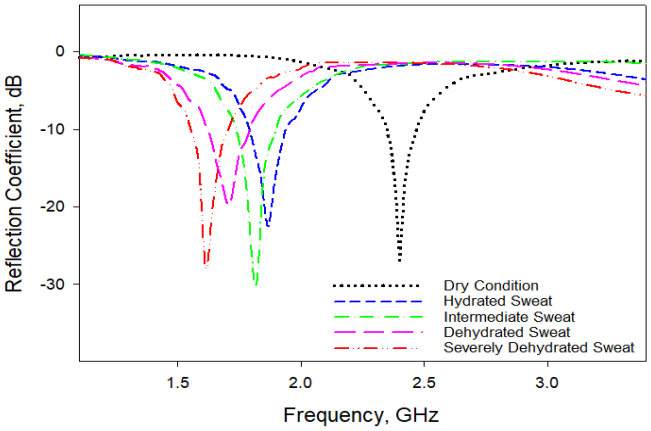
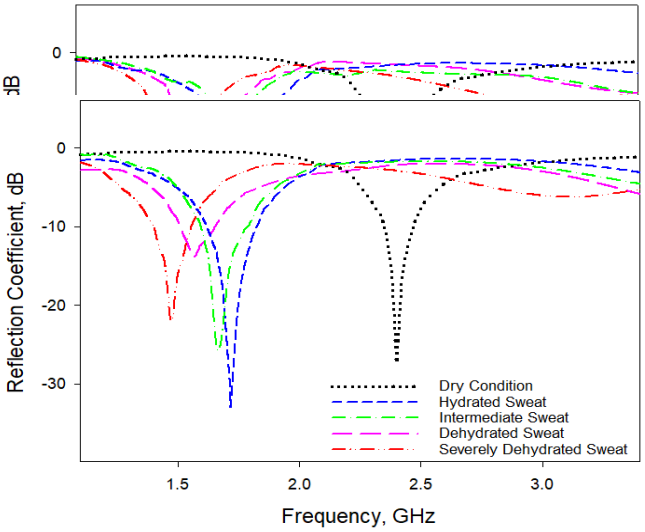


Fig. 9. Measured reflection coefficients under one-droplet condition.

Fig. 10. Measured reflection coefficients under two-droplet condition.

Fig. 11. Measured reflection coefficients under three-droplet condition.

At the one-droplet condition, as shown in Fig. 9, the reflection coefficient exhibited small but distinct shifts across all sweat categories. The antenna-based sensor response showed noticeable changes in resonant frequency with the reflection coefficient shifting more significantly for the dehydrated and severely dehydrated sweat samples compared to the hydrated and intermediate ones. These results indicate that even a small sweat volume is sufficient to alter the antenna-based sensor's impedance characteristics, signifying the



sensitivity of the CPW structure to surface dielectric perturbations. The observed resonance shift occurs due to the localized change in effective permittivity at the sensing region, where the absorbed sweat modifies the electromagnetic field distribution along the coplanar gap.

At the two-droplet condition, depicted in Fig. 10, the antenna-based sensor exhibited more pronounced frequency shifts for all sweat categories. The hydrated, intermediate, dehydrated, and severely dehydrated sweat recorded resonant

frequencies of 1.774, 1.728, 1.636, and 1.544 GHz, respectively, corresponding to frequency shifts of 0.626, 0.672, 0.764, and 0.856 GHz relative to the dry condition. The percentage relative frequency shifts were 26.08, 28.00, 31.83, and 35.67 percent, respectively. These results demonstrate that increasing the droplet volume enhances the dielectric loading effect on the antenna-based sensor surface, which increases the effective permittivity within the coplanar region. The presence of additional sweat volume increases electromagnetic field confinement, resulting in a stronger perturbation of the resonant mode. The progressive increase in both frequency shift and reflection magnitude confirms the antenna-based sensor's high responsiveness to variations in sweat concentration and volume.

Furthermore, at the three-droplet condition, as shown in Fig. 11, the antenna-based sensor response became even more pronounced compared to the previous conditions. The reflection coefficient exhibited substantial frequency displacement across all sweat types, indicating stronger interaction between the electromagnetic fields and the wetted substrate. These results indicate that the accumulated droplets increase dielectric loading on the substrate surface, enhancing coupling efficiency and improving the antenna-based sensor's ability to detect subtle variations in sweat composition and hydration state.

The overall performance of FS and PRFS across the four sweat categories and droplet conditions is illustrated in Fig. 12. and Fig. 13. These figures demonstrate a consistent trend: as the number of droplets increases from one to three, the antenna-based sensor exhibits a corresponding increase in both FS and PRFS for all sweat categories. Under the three-droplet condition, the dehydrated and severely dehydrated samples exhibit the largest frequency deviations, with FS values increasing to approximately 0.83 and 0.92 GHz and PRFS reaching about 34.71 % to 38.63 % respectively. In contrast, the hydrated and intermediate samples show comparatively smaller shifts, with FS values of roughly 0.68 to 0.74 GHz and PRFS between 28.38 % and 30.88 %. This trend reflects the influence of ionic concentration on the effective dielectric properties at the sensing region, where higher NaCl content enhances the electromagnetic perturbation at the antenna-based sensor substrate interface. The consistent increase in FS and PRFS with droplet count validates the ability of the CPW antenna-based sensor to detect hydration level changes driven by both sweat composition and deposited volume, demonstrating a stable and repeatable response across three-droplet conditions.

To further quantify the responsiveness of the CPW antenna-based sensor toward varying sweat compositions, a volume-based sensitivity analysis was conducted using the resonant frequency shift per unit deposited sweat volume. Fig. 14 presents the calculated sensitivity for the four sweat categories under one-, two-, and three-droplet conditions. At the one-droplet condition, the antenna-based sensor exhibits the highest sensitivity for all sweat categories, indicating strong responsiveness to small sweat volumes. The sensitivity increases progressively from hydrated to severely dehydrated sweat, with hydrated and intermediate sweat showing lower sensitivity values of approximately 10.68 and 11.60 GHz mL^{-1}, respectively, while dehydrated and severely dehydrated sweat produce higher sensitivities of about 13.90 and 15.74 GHz mL^{-1}. This behaviour demonstrates that even minimal sweat deposition is sufficient to induce a measurable and distinct frequency shift, highlighting the capability of the proposed antenna-based sensor to detect early-stage perspiration.

As the droplet count increases from one to three, a gradual reduction in sensitivity is observed across all sweat categories. For example, the sensitivity of hydrated sweat decreases from approximately 10.68 GHz mL^{-1} under one droplet to about 4.54 GHz mL^{-1} under three droplets, while severely dehydrated sweat decreases from 15.74 GHz mL^{-1} to 6.18 GHz mL^{-1}. This reduction is attributed to progressive saturation of the sensing region, where additional sweat volume spreads beyond the highest electric-field zone, resulting in diminishing incremental perturbations of the electromagnetic field and hence smaller frequency shifts per unit volume.

Despite this reduction, the antenna-based sensor maintains a consistent and monotonic response across all droplet conditions. Notably, severely dehydrated sweat consistently exhibits the highest sensitivity, followed by dehydrated, intermediate, and hydrated sweat, preserving the same hydration-level ranking for one-, two-, and three-droplet measurements. This consistency confirms that the antenna-based sensor response remains governed by sweat composition rather than volume-induced randomness. Collectively, these results indicate that the proposed CPW antenna-based sensor is highly sensitive to small amounts of sweat while maintaining reliable and distinguishable responses as sweat volume increases. The combined influence of ionic concentration and volume-dependent electromagnetic loading ensures robust detection across varying perspiration levels, validating volume-based sensitivity as a reliable quantitative indicator for sweat-based hydration monitoring.

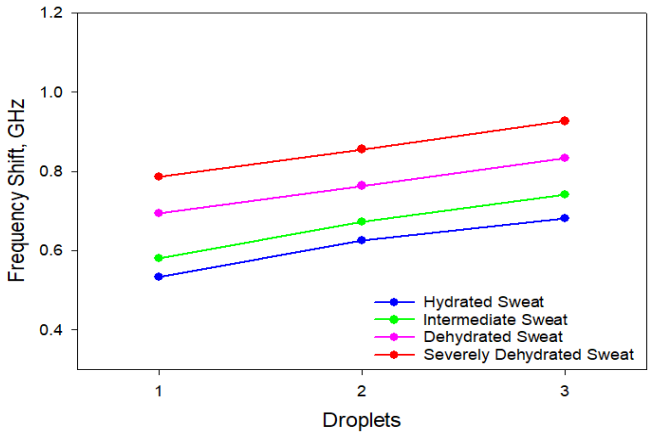


Fig. 12. FS under one-, two-, and three-droplet conditions.

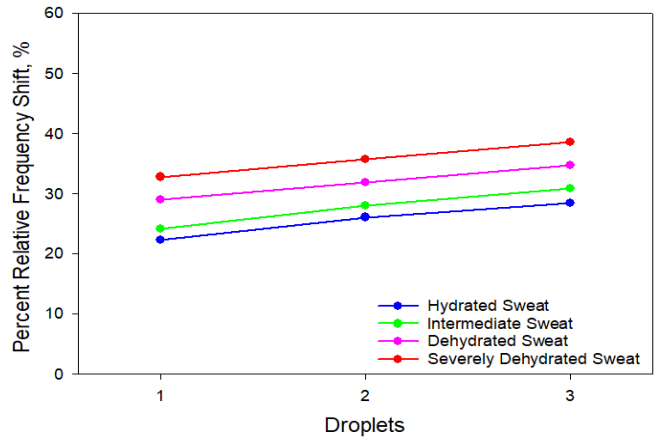


Fig. 13. PRFS under one-, two-, and three-droplet conditions.

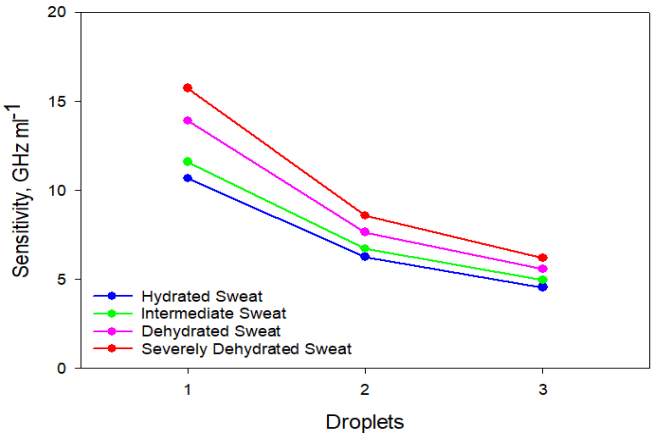


Fig. 14. S under one-, two-, and three-droplet conditions.

C. Comparative Analysis of Sensitivity Performance with Previous Studies

The development of antenna-based sensors for hydration monitoring remains an emerging field, with relatively few studies dedicated to this application. Most existing studies have primarily focused on microstrip patch antennas as wearable antenna-based sensors for monitoring hydration levels. One such study, presented in [33], investigates the use of patch antenna-based sensor with varying dielectric constant of paper substrates. However, this research is confined to simulations, which limits the potential for direct comparison with experimental results, thereby restricting a comprehensive assessment of the antenna-based sensor performance. In a different approach, the study in [35] examines a CPW antenna-based sensor that utilizes FR4 as a substrate and filter paper as a superstrate to detect and analyze sweat composition. However, this study focuses on the transmission coefficient, which complicates direct comparisons with the reflection coefficient parameter used in evaluating the performance of the proposed CPW antenna-based sensor.

Another relevant study is found in [34], where a patch antenna-based sensor is designed with slots that function as the sensing area for sweat absorption. This research, which employs filter paper as the substrate material, offers a closer point of comparison due to its similar materials and objectives. The antenna-based sensor, measuring 60 x 50 mm, features two square slots, each 11 mm in length specifically designed to absorb sweat. Among the few studies, the research in [34] is particularly relevant for comparing the sensitivity performance of the conventional antenna-based sensor with the proposed CPW antenna-based sensor. To facilitate this comparison, the FS, PRFS and S metrics as defined in Equation (1) – (3) are utilized. Additionally, the percent relative frequency shift enhancement (PRFSE) and sensitivity enhancement (SE) metrics are employed to quantify the performance improvement of the proposed CPW antenna-based sensor relative to the conventional design in [34]. The corresponding equations adopted from [42] are given as follows:

$$PRFSE = \frac{PRFS_{proposed}}{PRFS_{conventional}} \tag{4}$$

$$SE = \frac{S_{proposed}}{S_{conventional}} \tag{5}$$

PRFSE is calculated using (4) quantifies the improvement in relative frequency response, while SE, calculated using (5) expresses the sensitivity enhancement of the proposed CPW antenna-based sensor relative to the conventional design.

TABLE III. RESONANT FREQUENCIES OF CONVENTIONAL AND PROPOSED ANTENNA-BASED SENSORS UNDER DRY AND SWEAT CONDITIONS

Antenna-Based Sensor	Size (mm)	Dry Condition (GHz)	0.05 % NaCl Concentration (GHz)	0.05 % NaCl Concentration (GHz)	0.5 % NaCl Concentration (GHz)	1.0 % NaCl Concentration (GHz)
Conventional [34]	60x50	2	1.7	Not Measured	1.58	1.56
Proposed	30x30	2.4	1.774	1.728	1.636	1.544

Based on Equations (1) – (5) and the data summarised in Table III, the FS, PRFS, PRFSE, S and SE of the conventional and proposed CPW antenna-based sensors are illustrated in Fig. 15, Fig. 16, Fig. 17, Fig. 18 and Fig. 19 respectively. The two-droplet condition is selected for comparison, as it corresponds to an identical deposited sweat volume for both the conventional and proposed antenna-based sensors, ensuring consistency and fairness in the performance evaluation across hydrated (0.05% NaCl), dehydrated (0.5% NaCl), and severely dehydrated (1% NaCl) conditions. As depicted in Fig. 15, the proposed CPW antenna-based sensor exhibits consistently larger FS values across all sweat conditions compared to the conventional antenna-based sensor, indicating stronger electromagnetic interaction with the deposited sweat volume. A similar improvement is observed in Fig. 16, where the PRFS values of the proposed CPW antenna-based sensor are significantly higher, confirming enhanced responsiveness to hydration-related changes. Specifically, the PRFS values for the conventional antenna-based sensor were 15 %, 21 %, and 22 % for hydrated, dehydrated, and severely dehydrated conditions, respectively. In contrast, the proposed CPW antenna-based sensor achieved superior PRFS values of 26.08 %, 31.83 %, and 35.66 % under the same conditions.

The PRFSE results illustrated in Fig. 17, further quantify these improvements, with the proposed CPW antenna-based sensor showing enhancements factors of 1.739, 1.516, and 1.621 for hydrated, dehydrated, and severely dehydrated sweat,

respectively. Notably, the largest relative improvement occurs under hydrated conditions, where the conventional antenna exhibits limited sensitivity due to the low ionic concentration of the sweat. This highlights the effectiveness of the proposed CPW structure in enhancing detection capability under low-contrast sensing scenarios. Next, Fig. 18 compares the volume-based sensitivity of both antenna-based sensors, defined as the resonant frequency shift per unit deposited sweat volume. The proposed CPW antenna-based sensor demonstrates higher sensitivity values of 6.26, 7.64, and 8.56 GHz mL^{-1} for hydrated, dehydrated, and severely dehydrated sweat, respectively, compared to 3.00, 4.20, and 4.40 GHz mL^{-1} for the conventional antenna-based sensor. This improvement reflects enhanced electromagnetic coupling between the sensing region of the proposed CPW antenna-based sensor and the deposited sweat, enabling more efficient conversion of volume variation into resonant frequency shift.

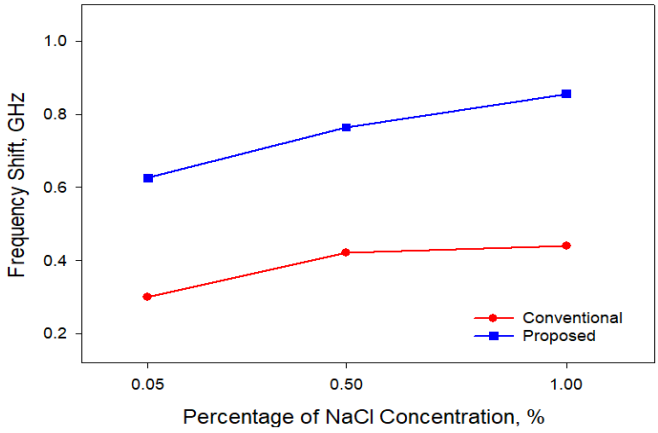


Fig. 15. FS comparison between conventional and proposed antenna-based sensors under two-droplet condition.

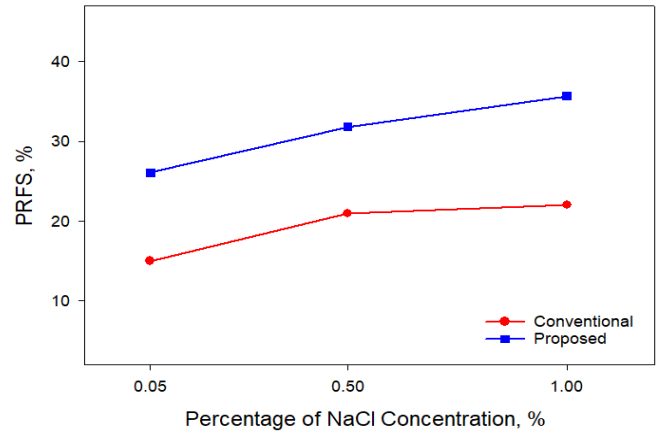


Fig. 16. PRFS comparison between conventional and proposed antenna-based sensors under two-droplet condition.

The corresponding sensitivity enhancement factors, shown in Fig. 19, further confirm this improvement, with SE values exceeding 2.0 for hydrated sweat and remaining above 1.8 for higher salinity conditions. Although severely dehydrated sweat produces the largest absolute frequency shifts, hydrated sweat exhibits the highest relative enhancement, demonstrating that the proposed CPW antenna-based sensor significantly improves detection capability under weak-loading conditions. This comparison confirms that the proposed CPW antenna-based sensor not only increases absolute sensitivity for highly saline sweat but also substantially enhances detection performance for low-salinity sweat, which is critical for early-stage dehydration monitoring.

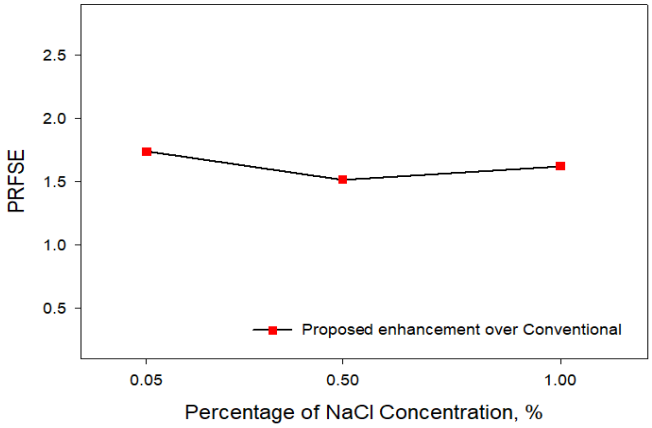


Fig. 17. PRFSE of the proposed CPW antenna-based sensor.

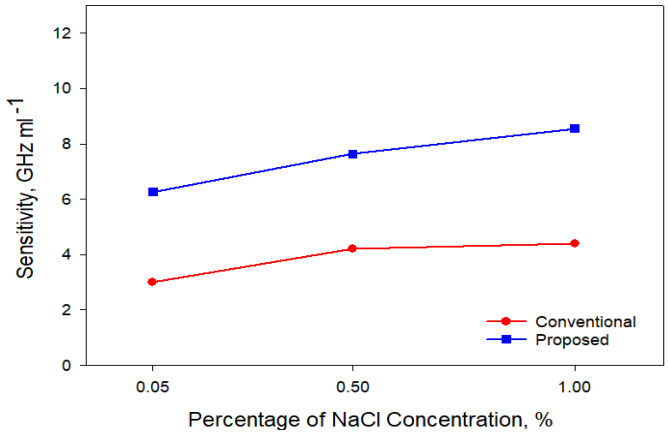


Fig. 18. S comparison between conventional and proposed antenna-based sensors under two-droplet condition.

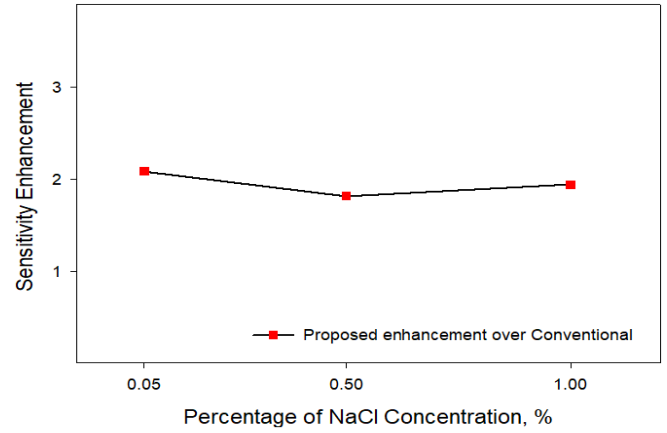


Fig. 19. SE of the proposed CPW antenna-based sensor.

IV. CONCLUSION

A paper-based CPW antenna-based sensor has been successfully designed, fabricated, and experimentally validated for sweat-based hydration monitoring. The proposed design exploits high absorbency and flexibility of filter paper to enable effective electromagnetic interaction between the antenna-based sensor and deposited sweat. Experimental results obtained using a controlled droplet deposition method indicate that different sweat compositions produce clearly separable resonant frequency shifts and reflection-coefficient responses, confirming that both ionic concentration and deposited sweat volume directly influence the antenna-based sensor behaviour. The CPW antenna-based sensor exhibits consistent FS and PRFS trends across one-, two-, and three-droplet conditions, indicating stable and repeatable performance under varying sweat volumes. Sensitivity analysis reveals that the antenna-based sensor is highly responsive even at low sweat volumes, with severely dehydrated sweat producing the largest frequency shift per unit volume due to its higher ionic content, while hydrated sweat yields smaller but clearly distinguishable responses. Compared with a conventional design, the proposed CPW antenna-based sensor demonstrates enhanced sensitivity and improved sensing performance under identical droplet conditions, highlighting the effectiveness of the CPW configuration and field-concentrated sensing region. The present study employs artificial sweat formulations to provide controlled and repeatable electrolyte conditions for sensitivity evaluation. While this approach enables systematic investigation of the antenna-based sensor response under well-defined hydration conditions, real human sweat may vary between individuals in terms of sweat rate, electrolyte concentration, and chemical composition. In addition, collecting sufficient sweat volume for controlled and repeatable measurements may require extended collection periods, as sweat generation rates vary between individuals. These factors may influence the antenna-based sensor response under practical operating conditions. Future work will therefore focus on validating the proposed antenna-based sensor using real human sweat samples and wearable on-body measurements to assess performance under realistic conditions involving body movement, continuous perspiration, and environmental variations. The integration of the proposed CPW antenna-based sensor with Internet of Things (IoT) platforms will also be explored as a future direction for wireless and continuous hydration monitoring, supported by its operation within the 2.4 GHz ISM band.

ACKNOWLEDGMENT

The authors gratefully acknowledge the assistance and support provided by the Antenna and Microwave Research Group (AMRG), Universiti Teknologi MARA Cawangan Pulau Pinang, and the Advanced Communication Engineering Center (ACE), Universiti Malaysia Perlis. The authors would also like to express their gratitude to the Institute of Postgraduate Studies (IPSIS), Universiti Teknologi MARA, for the financial support provided for this research.

REFERENCES

[1] K. Guk *et al.*, "Evolution of Wearable Devices with Real-Time Disease Monitoring for Personalized Healthcare," *Nanomaterials*, vol. 9, 2019, doi: 10.3390/nano9060813.

[2] G. Yang, G. Pang, Z. Pang, Y. Gu, M. Mantysalo, and H. Yang, "Non-Invasive Flexible and Stretchable Wearable Sensors with Nano-Based Enhancement for Chronic Disease Care," *IEEE Rev. Biomed. Eng.*, vol. 12, pp. 34–71, 2019, doi: 10.1109/RBME.2018.2887301.

[3] C. Lafaye *et al.*, "Real-Time Smart Multisensing Wearable Platform for Monitoring Sweat Biomarkers During Exercise," in *IEEE Biomedical Circuits and Systems Conference: Intelligent Biomedical Systems, BioCAS 2022*, Institute of Electrical and Electronics Engineers Inc., 2022, pp. 173–177. doi: 10.1109/BioCAS54905.2022.9948565.

[4] X. Wang, Y. Ma, M. Zeng, and P. Niu, "Single-Gland-Level Sweat Sampling: A Theoretical and Computational Approach Toward Improved Biomarker Accuracy in Wearable Sensors," *IEEE Trans. Biomed. Eng.*, vol. 73, pp. 1202–1209, Mar. 2026, doi: 10.1109/TBME.2025.3600238.

[5] T. H. Nguyen, T. L. H. Nguyen, and T. P. Vuong, "A Printed Wearable Dual Band Antenna for Remote Healthcare Monitoring Device," in *IEEE-RIVF International Conference on Computing and Communication Technologies : Danang, Vietnam, March 20-22, 2019.*, 2019. doi: 10.1109/RIVF.2019.8713714.

[6] X. F. Teng, C. C. Y. Poon, Y. T. Zhang, and P. Bonato, "Wearable Medical Systems for p-Health," *IEEE Rev. Biomed. Eng.*, vol. 1, pp. 62–74, 2008, doi: 10.1109/RBME.2008.2008248.

[7] A. Lymberis and R. Paradiso, "Smart Fabrics and Interactive Textile Enabling Wearable Personal Applications: R&D State of the Art and Future Challenges," in *30th Annual International Conference of the IEEE Engineering in Medicine and Biology Society*, 2008. doi: 10.1109/IEMBS.2008.4650403.

[8] A. B. Amado-Rey, A. C. Goncalves Seabra, and T. Stieglitz, "Towards Ultrasound Wearable Technology for Cardiovascular Monitoring: From Device Development to Clinical Validation," *IEEE Rev. Biomed. Eng.*, vol. 18, pp. 93–112, 2025, doi: 10.1109/RBME.2024.3410399.

[9] D. K. Vo and K. T. L. Trinh, "Advances in Wearable Biosensors for Healthcare: Current Trends, Applications, and Future Perspectives," *Biosensors (Basel).*, vol. 14, no. 11, 2024, doi: 10.3390/bios14110560.

[10] N. F. A. Ibrahim *et al.*, "A Comprehensive Review of the Recent Developments in Wearable Sweat-Sensing Devices," Oct. 01, 2022, *MDPI*. doi: 10.3390/s22197670.

[11] Y. Qiao, L. Qiao, Z. Chen, B. Liu, L. Gao, and L. Zhang, "Wearable Sensor for Continuous Sweat Biomarker Monitoring," *Chemosensors*, vol. 10, no. 7, 2022, doi: 10.3390/chemosensors10070273.

[12] M. S. Islam, S. Cha, W. Cai, M. Ferdoushi, and Y. Khan, "A Wearable Sweat Rate Sensor With Adaptive Sweat Ion Concentration Calibration," *IEEE Sens. Lett.*, vol. 9, no. 7, 2025, doi: 10.1109/LSENS.2025.3579329.

[13] M. Chung, G. Fortunato, and N. Radacsi, "Wearable Flexible Sweat Sensors for Healthcare Monitoring: A Review," *J. R. Soc. Interface*, vol. 16, no. 159, 2019, doi: 10.1098/rsif.2019.0217.

[14] C. Legner, U. Kalwa, V. Patel, A. Chesmore, and S. Pandey, "Sweat Sensing in the Smart Wearables Era: Towards Integrative, Multifunctional and Body-Compliant Perspiration Analysis," *Sens. Actuators A Phys.*, vol. 296, pp. 200–221, Sep. 2019, doi: 10.1016/j.sna.2019.07.020.

[15] F. Gao *et al.*, "Wearable and Flexible Electrochemical Sensors for Sweat Analysis: A Review," *Microsyst. Nanoeng.*, vol. 9, no. 1, Dec. 2023, doi: 10.1038/s41378-022-00443-6.

[16] J. Zhou, D. Men, and X. E. Zhang, "Progress in Wearable Sweat Sensors and Their Applications," *Chinese Journal of Analytical Chemistry*, vol. 50, no. 2, pp. 87–96, Feb. 2022, doi: 10.1016/j.cjac.2021.11.004.

[17] A. J. Bandodkar, W. J. Jeang, R. Ghaffari, and J. A. Rogers, "Wearable Sensors for Biochemical Sweat Analysis," *Annual Review of Analytical Chemistry 2019*, vol. 12, pp. 1–22, 2019, doi: 10.1146/annurev-anchem-061318.

[18] K. K. Yeung, T. Huang, Y. Hua, K. Zhang, M. M. F. Yuen, and Z. Gao, "Recent Advances in Electrochemical Sensors for Wearable

Sweat Monitoring: A Review," *IEEE Sens. J.*, vol. 21, no. 13, pp. 14522–14539, Jul. 2021, doi: 10.1109/JSEN.2021.3074311.

[19] R. Priyadharshni, K. Vijaya Kumar, V. Parvathy, and S. Balanethiram, "Comparative Study of TFET Architectures for Label-Free Breast Cancer Biomarker Detection in Saliva and Serum samples," in *7th IEEE International Conference on Emerging Electronics, ICEE 2025*, Institute of Electrical and Electronics Engineers Inc., 2025. doi: 10.1109/ICEE67165.2025.11409951.

[20] H. Ali, S. Johri, C. Semaan, and R. Prakash, "Screening Alzheimer's Disease Biomarkers Using a Portable Antibody Functionalized Bioanalyzer Platform and Novel Saliva Testing Strategies," in *IEEE Sensors*, Institute of Electrical and Electronics Engineers (IEEE), Jan. 2025, pp. 1–4. doi: 10.1109/sensors59705.2025.11330428.

[21] A. J. Bandodkar and J. Wang, "Non-Invasive Wearable Electrochemical Sensors: A Review," *Trends Biotechnol.*, vol. 32, no. 7, pp. 363–371, 2014, doi: 10.1016/j.tibtech.2014.04.005.

[22] Y. Mengistu, M. Pham, H. M. Do, and W. Sheng, "AutoHydrate: A Wearable Hydration Monitoring System," in *IEEE International Conference on Intelligent Robots and Systems*, Institute of Electrical and Electronics Engineers Inc., Nov. 2016, pp. 1857–1862. doi: 10.1109/IROS.2016.7759295.

[23] Y. Yang and W. Gao, "Wearable and Flexible Electronics for Continuous Molecular Monitoring," *Chem. Soc. Rev.*, vol. 48, no. 6, pp. 1465–1491, Mar. 2019, doi: 10.1039/c7cs00730b.

[24] J. Wang, Z. Zilic, and Y. Shu, "Evaluation of an RF Wearable Device for Non-Invasive Real-Time Hydration Monitoring," in *2017 IEEE 14th International Conference on Wearable and Implantable Body Sensor Networks, BSN 2017*, Institute of Electrical and Electronics Engineers Inc., May 2017, pp. 91–94. doi: 10.1109/BSN.2017.7936015.

[25] S. M. Shirreffs, "The Importance of Good Hydration for Work and Exercise Performance," *Nutr. Rev.*, vol. 63, no. 6, pp. 14–21, 2005, doi: 10.1301/nr.2005.jun.S14.

[26] Susan M. Kleiner, "Water: An Essential but Overlooked Nutrient," *J. Am. Diet. Assoc.*, vol. 99, no. 2, pp. 200–206, 1999, doi: 10.1016/S0002-8223(99)00048-6.

[27] E. Blancaflor, M. R. A. D. Cruz, N. M. E. Dionisio, J. M. V. Espanola, J. W. J. Maranan, and J. M. Miraflores, "An IoT Design of a Dehydration Indicator System Based on Urine Color," in *2022 5th International Conference on Computing and Big Data, ICCBD 2022*, Institute of Electrical and Electronics Engineers Inc., 2022, pp. 118–122. doi: 10.1109/ICCBD56965.2022.10080279.

[28] L. A. Popowski, R. A. Oppliger, G. P. Lambert, R. F. Johnson, A. K. Johnson, and C. V Gisolfi, "Blood and Urinary Measures of Hydration Status During Progressive Acute Dehydration," *Med. Sci. Sports Exerc*, vol. 33, no. 5, pp. 747–753, 2001, doi: 10.1097/00005768-200105000-00011.

[29] Armstrong. Lawrence E. *et al.*, "Urinary Indices of Hydration Status," *International Journal of Sport Nutrion*, vol. 4, pp. 265–279, 1994, doi: 10.1123/ijsn.4.3.265.

[30] U. Farooq *et al.*, "Design of a 1×4 CPW Microstrip Antenna Array on PET Substrate for Biomedical Applications," in *2019 IEEE International Symposium on Antennas and Propagation and USNC-URSI Radio Science Meeting*, IEEE, 2019. doi: 10.1109/APUSNCURSINRSM.2019.8889355.

[31] S. S. Dhanabalan *et al.*, "Flexible Compact System for Wearable Health Monitoring Applications," *Computers and Electrical Engineering*, vol. 102, Sep. 2022, doi: 10.1016/j.compeleceng.2022.108130.

[32] H. K. Raad, H. M. Al-Rizzo, A. Isaac, and A. I. Hammoodi, "A Compact Dual Band Polyimide Based Antenna for Wearable and Flexible Telemedicine Devices," *Progress In Electromagnetics Research C*, vol. 63, pp. 153–161, 2016, doi: 10.2528/PIERC16010707.

[33] S. H. Rakib, M. T. Reza, and Md. F. Islam, "Design of Microstrip Patch Sensor for Non-Invasive Body Electrolyte Monitoring," in *2020 IEEE Region 10 Symposium (TENSYMP) : 5-7 June 2020, Dhaka, Bangladesh*, 2020. doi: 10.1109/TENSYMP50017.2020.9230891.

[34] A. R. Eldamak and E. C. Fear, "Conformal and Disposable Antenna-Based Sensor for Non-Invasive Sweat Monitoring," *Sensors*, vol. 18, no. 12, Dec. 2018, doi: 10.3390/S18124088.

[35] M. M. Y. R. Riad and A. R. Eldamak, "Coplanar Waveguide Based Sensor Using Paper Superstrate for Non-Invasive Sweat Monitoring," *IEEE Access*, vol. 8, pp. 177757–177766, 2020, doi: 10.1109/ACCESS.2020.3027033.

[36] N. S. Shagle *et al.*, "Design and Fabrication of Paper-based Stretchable Sensor for Respiration Monitoring," in *IEEE Sensors*, Institute of Electrical and Electronics Engineers Inc., 2021. doi: 10.1109/SENSORS47087.2021.9639648.

[37] Z. Li, S. Tian, J. Tang, W. Yang, T. Hong, and H. Zhu, "High-Sensitivity Differential Sensor for Characterizing Complex Permittivity of Liquids Based on LC Resonators," *Sensors*, vol. 24, no. 15, Aug. 2024, doi: 10.3390/s24154877.

[38] A. Ebrahimi, W. Withayachumnankul, S. Al-Sarawi, and D. Abbott, "High-Sensitivity Metamaterial-Inspired Sensor for Microfluidic Dielectric Characterization," *IEEE Sens. J.*, vol. 14, no. 5, pp. 1345–1351, 2014, doi: 10.1109/JSEN.2013.2295312.

[39] A. Mena-Bravo and M. D. Luque de Castro, "Sweat: A Sample with Limited Present Applications and Promising Future in Metabolomics," *J. Pharm. Biomed. Anal.*, vol. 90, pp. 139–147, Mar. 2014, doi: 10.1016/j.jpba.2013.10.048.

[40] J. Haakma, E. Peri, S. Turco, E. Pelssers, J. Den Toonder, and M. Mischi, "A model for Digital Sweat Sensing Devices," in *MELECON 2022 - IEEE Mediterranean Electrotechnical Conference, Proceedings*, Institute of Electrical and Electronics Engineers Inc., 2022, pp. 715–719. doi: 10.1109/MELECON53508.2022.9842932.

[41] A. R. Eldamak, S. Thorson, and E. C. Fear, "Study of the Dielectric Properties of Artificial Sweat Mixtures at Microwave Frequencies," *Biosensors (Basel).*, vol. 10, no. 6, Jun. 2020, doi: 10.3390/BIOS10060062.

[42] J. Yeo and J. I. Lee, "Slot-Loaded Microstrip Patch Sensor Antenna for High-Sensitivity Permittivity Characterization," *Electronics (Switzerland)*, vol. 8, no. 5, May 2019, doi: 10.3390/electronics8050502.